

# On the application of the spectral projected gradient method in image segmentation

Laura Antonelli · Valentina De Simone · Daniela di Serafino

May 22, 2015

**Abstract** We investigate the application of the non-monotone spectral projected gradient (SPG) method to a region-based variational model for image segmentation. We consider a “discretize-then-optimize” approach and solve the resulting nonlinear optimization problem by an alternating minimization procedure that exploits the SPG2 algorithm by Birgin, Martínez and Raydan (SIAM J. Optim., 10(4), 2000). We provide a convergence analysis and perform numerical experiments on several images, showing the effectiveness of this procedure.

**Keywords** Image segmentation · Region-based variational model · Spectral Projected Gradient

**Mathematics Subject Classification (2010)**  
68U10 · 65K05 · 90C30

---

Work partially supported by INdAM-GNCS (2014 Project *First-order optimization methods for image restoration and analysis*; 2015 Project *Numerical Methods for Nonconvex/Nonsmooth Optimization and Applications*) and by MIUR (FIRB 2010 Project n. RBFR106S1Z002).

---

L. Antonelli  
Institute for High-Performance Computing and Networking (ICAR), CNR, via P. Castellino 111, I-80131 Naples, Italy  
E-mail: laura.antonelli@na.icar.cnr.it

D. di Serafino  
Department of Mathematics and Physics, Second University of Naples, viale A. Lincoln 5, I-81100 Caserta, Italy  
E-mail: daniela.diserafino@unina2.it

V. De Simone  
Department of Mathematics and Physics, Second University of Naples, viale A. Lincoln 5, I-81100 Caserta, Italy  
E-mail: valentina.desimone@unina2.it

## 1 Introduction: background and motivations

Image segmentation is the process of partitioning an image into regions that are “homogeneous” according to some feature, such as intensity, texture or colour. This process is generally aimed at identifying objects in the image, thus it plays a fundamental role in computer vision, e.g., for object detection, recognition, measurement and tracking. Many successful methods for image segmentation are based on variational models where the regions of the desired partition, or their edges, are obtained by minimizing suitable cost functionals (see, e.g., [14, 9, 23, 26] and the references therein).

In this work we consider a region-based variational model by Chan, Esedoğlu and Nikolova [13], henceforth referred to as CEN model, which has been obtained by applying a suitable relaxation to the Chan-Vese (CV) model [15] with the aim of overcoming minimization difficulties associated with its non-convexity. The CV model is actually the Mumford-Shah one [27] restricted to the case of piecewise constant two-phase segmentation; its level-set formulation reads as follows:

$$\min_{c_1, c_2, \phi} E_{CV}(c_1, c_2, \phi), \quad (1)$$

where

$$\begin{aligned} E_{CV}(c_1, c_2, \phi) = & \int_{\Omega} |\nabla H(\phi(x))| dx \\ & + \lambda \left( \int_{\Omega} H(\phi(x)) (c_1 - \bar{u}(x))^2 dx \right. \\ & \left. + \int_{\Omega} (1 - H(\phi(x))) (c_2 - \bar{u}(x))^2 dx \right). \end{aligned} \quad (2)$$

Here  $\Omega \subset \mathbb{R}^2$  is an open bounded set with Lipschitz boundary (generally a rectangle),  $\bar{u}(x) : \Omega \rightarrow \mathbb{R}$  represents the image to be segmented,  $H$  is the Heaviside function,  $\phi : \Omega \rightarrow \mathbb{R}$  is a Lipschitz-continuous function whose zero level set represents the boundary  $\partial\Omega$  of a set

$\Sigma \subset \Omega$ ,  $c_1, c_2 \in \mathbb{R}$ , and  $\lambda > 0$  is a suitable regularization parameter. Solving (1) means finding the best approximation to  $\bar{u}(x)$  among all the functions that take only two values;  $c_1$  and  $c_2$  represent these values, while  $\Sigma$  and  $\Omega \setminus \Sigma$  are the sets where they are taken, which provide a two-phase partition of  $\Omega$ . The first term in the right-hand side of (2) is a regularization term, which penalizes the size of  $\partial \Sigma$ . For any fixed  $\phi$ , the values of  $c_1$  and  $c_2$  that minimize  $E_{CV}$  are given by

$$\begin{aligned} c_1 &= \frac{\int_{\Omega} \bar{u}(x) H(\phi(x)) dx}{\int_{\Omega} H(\phi(x)) dx}, \\ c_2 &= \frac{\int_{\Omega} \bar{u}(x) (1 - H(\phi(x))) dx}{\int_{\Omega} (1 - H(\phi(x))) dx}, \end{aligned} \quad (3)$$

i.e., by the mean values of  $\bar{u}(x)$  in the regions  $\Sigma$  and  $\Omega \setminus \Sigma$ . Therefore, a natural approach to solve problem (1) is to alternate between the computation of  $c_1$  and  $c_2$  through (3) and the minimization of  $E_{CV}(c_1, c_2, \phi)$  with respect to  $\phi$ . This minimization is usually performed by using a gradient-descent scheme, where the first variation of  $E_{CV}(c_1, c_2, \phi)$  is computed by using a smooth regularization of the Heaviside function [15]. However, because of the non-convexity of the functional  $E_{CV}$  with respect to  $\phi$ , this method may get stuck into local minima, thus providing poor segmentations.

In order to overcome the previous problem, a convex relaxation approach is used in the CEN model, which is based on the idea of removing the constraint that  $\bar{u}(x)$  be approximated by functions taking only two values. Specifically, in [13, Theorem 2] it is proved that, for any given  $(c_1, c_2)$ , a global minimizer for the piecewise constant two-phase Mumford-Shah model can be obtained by solving the following convex problem:

$$\begin{aligned} \min_u & E_{CEN}(c_1, c_2, u), \\ \text{s.t. } & 0 \leq u \leq 1, \end{aligned} \quad (4)$$

where

$$\begin{aligned} E_{CEN}(c_1, c_2, u) &= \int_{\Omega} |\nabla u| dx \\ &+ \lambda \left( \int_{\Omega} u(x) (c_1 - \bar{u}(x))^2 dx \right. \\ &\left. + \int_{\Omega} (1 - u(x)) (c_2 - \bar{u}(x))^2 dx \right), \end{aligned} \quad (5)$$

and by taking

$$\Sigma = \{x \in \Omega : u(x) \geq \mu\}, \quad (6)$$

for almost any  $\mu \in (0, 1)$ .

Different methods have been proposed to solve problem (4). In [13] the constraint  $0 \leq u \leq 1$  is enforced by using a penalty term and then applying the gradient-descent technique to the resulting unconstrained problem. Regularized versions of both  $|\nabla u|$  and the penalty term are used to deal with their non-differentiability.

A penalty approach, combined with a suitable splitting of the resulting energy functional, is also used in [9]. In this case, the minimization is performed by exploiting the dual formulation of the TV norm and adding a regularization term that allows the application of an alternating solution procedure, based on a semi-implicit gradient-descent algorithm and an explicit minimization formula [1]. As observed in [23], the previous methods may introduce too much regularization, possibly yielding the elimination of fine segmentation details. Furthermore, when explicit discretizations of the gradient flow equation are used, the resulting numerical methods are generally slow, because of the time step limitations imposed by stability conditions.

An approach that avoids regularization is based on the application of the Split Bregman (SB) method [23]. In this case, problem (4) is splitted into easier subproblems that can be efficiently solved within an alternating minimization scheme. The convergence of the SB method has been proved when the subproblems are solved exactly [24, 29]; however, it has been observed that approximate solutions can be used in practice without deteriorating convergence speed [23]. Furthermore, in [23] it has been shown that this approach outperforms the duality-based algorithm described in [9]. Another approach that exploits the dual formulation of the TV norm without introducing regularization terms has been proposed in [31]. In that work problem (4) is reformulated as a saddle-point one and solved by the first-order primal-dual method described in [12], which alternates minimizations over the primal and dual variables. We observe that alternating minimization methods for problem (4), or for variants of it, can be derived in the general context of Lagrangian methods (see, e.g., [30, 26]). There are indeed strong connections between the alternating direction method of multipliers and the SB method, as shown in [20, 29].

We also note that a relaxation of the CV model which is convex with respect to all its variables has been proposed in [10]. More precisely, the CV model has been approximated by a sequence of convex problems obtained by using a suitable reformulation of the original problem and a technique for embedding the resulting problem into a higher-dimensional space. The convex problems can be written as saddle-point ones and solved by using the aforementioned primal-dual method of [12]. However, we do not consider this approach, since the results reported in [10] show that its computational cost can be very high. An interesting discussion on convex relaxations of non-convex functionals used in image processing can be found in [28].

In this article we investigate the application of the nonmonotone spectral projected gradient (SPG) method,

within an alternating minimization procedure, to the CEN model. The interest for the SPG method is due to its faster convergence with respect to classical gradient projection methods, which results from the combination of the spectral properties of the Barzilai and Borwein (BB) steplength [2] with the nonmonotone line-search technique by Grippo, Lampariello and Lucidi (GLL) [25]. We note that the idea of using steplengths related somehow to the spectrum of the Hessian of the objective function, in order to speedup the convergence of gradient methods, has gained widespread acceptance in the last years; therefore, an increasing amount of work has been devoted to designing and applying new gradient methods that employ such steplengths (see, e.g., [6, 8, 17–19, 21, 22, 33]). In the context of image processing, the BB steplength has been used, e.g., in [32] to accelerate Chambolle’s gradient projection method for total variation image restoration [11]. In this case, the nonmonotone line-search technique by Dai and Fletcher [16] has been applied to ensure global convergence. Notice that the use of the BB steplength together with a nonmonotone line-search technique allows to overcome the limitations on the steplength required by classical explicit gradient-descent algorithms. On the other hand, the application of the SPG method requires some regularization of the TV term; however, we did not experience any drawbacks with using a small amount of regularization in our experiments (see Section 4).

We consider a “discretize-then-optimize” approach, i.e., we first consider a discretization of the CEN model and then solve the resulting optimization problem. We focus of the SPG2 algorithm proposed in [4]. The  $k$ -th iteration of our minimization procedure consists of two steps:

- computation of an approximation  $u^k$  to  $u$  by applying an SPG2 step, with a suitable GLL-type line search, to the discretized CEN functional where  $c_1$  and  $c_2$  are equal to the previously computed values  $c_1^{k-1}$  and  $c_2^{k-1}$ ;
- computation of  $c_1^k$  and  $c_2^k$  by exact minimization, by using a discrete version of (3) where  $u$  is set equal to  $u^k$ .

This method is proved to be globally convergent and its effectiveness is illustrated through numerical experiments on several test problems.

This paper is organized as follows. In Section 2 we provide a discrete formulation of the CEN model. In Section 3 we describe our SPG-based minimization algorithm and prove its convergence. In Section 4 we discuss the results of numerical experiments performed by applying our algorithm to several images. We also make a comparison with the SPG2 algorithm and with the

SB technique presented in [23]. Finally, in Section 5, we draw some conclusions.

## 2 Discrete formulation

The image domain  $\Omega$  is discretized by using an  $m \times n$  grid of pixels

$$\Gamma = \{(i, j) : 0 \leq i \leq m-1, 0 \leq j \leq n-1\}.$$

We identify each pixel with its center and denote by  $v_{i,j}$  the value in  $(i, j)$  of any function  $v$  defined in  $\Omega$ . Now we introduce some finite-difference operators that are useful to present the discretization of the functional (5) over the grid  $\Gamma$ . For any  $v_{i,j}$  with  $(i, j) \in \Gamma$ , we set

$$\begin{aligned}\delta_+^x v_{i,j} &= v_{i+1,j} - v_{i,j}, & \delta_+^y v_{i,j} &= v_{i,j+1} - v_{i,j}, \\ \delta_-^x v_{i,j} &= v_{i,j} - v_{i-1,j}, & \delta_-^y v_{i,j} &= v_{i,j} - v_{i,j-1},\end{aligned}$$

where we assume

$$\begin{aligned}v_{i-1,j} &= v_{i,j} \text{ for } i = 0, & v_{i,j-1} &= v_{i,j} \text{ for } j = 0, \\ v_{i+1,j} &= v_{i,j} \text{ for } i = m-1, & v_{i,j+1} &= v_{i,j} \text{ for } j = n-1,\end{aligned}$$

i.e., we define by replication the values of  $v$  with indices outside  $\Gamma$ . To discretize the total variation term in (5) we proceed as in [11]; however, in order to deal with non-differentiability, we use a classical regularization of  $|\nabla u|$ , i.e., we set

$$|\nabla u|_{i,j} = \sqrt{(\delta_+^x u_{i,j})^2 + (\delta_+^y u_{i,j})^2} + \varepsilon,$$

where  $\varepsilon$  is a small positive parameter. Then we consider the following discretization of the functional  $E_{\text{CEN}}$ :

$$\begin{aligned}E(c_1, c_2, u) &= \sum_{i,j} |\nabla u|_{i,j} \\ &\quad + \lambda \sum_{i,j} \left( (c_1 - \bar{u}_{i,j})^2 u_{i,j} + (c_2 - \bar{u}_{i,j})^2 (1 - u_{i,j}) \right),\end{aligned}$$

where the indices  $i$  and  $j$  in the sum run from 0 to  $m-1$  and from 0 to  $n-1$ , respectively.

Obviously, the function  $E(c_1, c_2, u)$  is continuously differentiable. Its derivatives take the following form:

$$\begin{aligned}\frac{\partial E}{\partial c_1} &= 2\lambda \sum_{i,j} (c_1 - \bar{u}_{i,j}) u_{i,j}, \\ \frac{\partial E}{\partial c_2} &= 2\lambda \sum_{i,j} (c_2 - \bar{u}_{i,j}) (1 - u_{i,j}), \\ \frac{\partial E}{\partial u_{i,j}} &= a_0 u_{i,j} \\ &\quad - a_1 u_{i+1,j} - a_2 u_{i-1,j} - a_3 u_{i,j+1} - a_4 u_{i,j-1} \\ &\quad + \lambda \left( (c_1 - \bar{u}_{i,j})^2 - (c_2 - \bar{u}_{i,j})^2 \right),\end{aligned} \tag{7}$$

where

$$\begin{aligned} a_1 &= \left( (\delta_+^x u_{i,j})^2 + (\delta_+^y u_{i,j})^2 + \varepsilon \right)^{-\frac{1}{2}}, \\ a_2 &= \left( (\delta_-^x u_{i,j})^2 + (\delta_+^y u_{i-1,j})^2 + \varepsilon \right)^{-\frac{1}{2}}, \\ a_4 &= \left( (\delta_+^x u_{i,j-1})^2 + (\delta_-^y u_{i,j})^2 + \varepsilon \right)^{-\frac{1}{2}}, \\ a_3 &= a_1, \quad a_0 = a_1 + a_2 + a_3 + a_4. \end{aligned} \quad (8)$$

By imposing  $\partial E / \partial c_1 = \partial E / \partial c_2 = 0$  we trivially obtain the values of  $c_1$  and  $c_2$  that minimize  $E$  for any fixed  $u$ :

$$\begin{aligned} c_1 &= \frac{\sum_{i,j} \bar{u}_{i,j} u_{i,j}}{\sum_{i,j} u_{i,j}}, \\ c_2 &= \frac{\sum_{i,j} \bar{u}_{i,j} (1 - u_{i,j})}{\sum_{i,j} (1 - u_{i,j})}. \end{aligned} \quad (9)$$

From (9) and  $0 \leq u_{i,j} \leq 1$  it follows that

$$u_{\min} \leq c_1, c_2 \leq u_{\max},$$

where  $u_{\min} = \min_{i,j} \bar{u}_{i,j}$  and  $u_{\max} = \max_{i,j} \bar{u}_{i,j}$ . Note also that (9) provides a discretization of (3) where  $H(\phi(x))$  has been replaced by  $u(x)$ .

In the following we focus on the solution of the problem

$$\begin{aligned} \min & E(c_1, c_2, u), \\ \text{s.t.} & 0 \leq u \leq 1, \\ & u_{\min} \leq c_1, c_2 \leq u_{\max}, \end{aligned} \quad (10)$$

where  $0 \leq u \leq 1$  is intended componentwise.

Henceforth, to simplify the notation, we denote by  $G$  the vector  $\nabla E$ , by  $G_c$  the vector with components  $\partial E / \partial c_1$  and  $\partial E / \partial c_2$ , and by  $G_u$  the vector with components  $\partial E / \partial u_{i,j}$  (we implicitly assume some ordering in the grid of pixels). For any vectors  $v$  and  $w$ , we use the notation  $(v, w)$  to denote  $(v^T, w^T)^T$ ; furthermore, we denote by  $\langle \cdot, \cdot \rangle$  the Euclidean inner product and by  $\| \cdot \|$  the induced vector norm.

### 3 An SPG-based alternating method for the discretized CEN model

We compute a solution to problem (10) by exploiting the SPG2 spectral projected gradient method proposed in [4] within an alternating minimization framework. Therefore, we first provide a short description of SPG2. Given a closed convex set  $X \subset \mathbb{R}^n$  and a function  $f : X \rightarrow \mathbb{R}$  that is continuously differentiable in an open set containing  $X$ , the SPG2 method attempts to compute a minimizer of  $f$  in  $X$  by building a sequence of approximate solutions as follows:

$$x^{k+1} = x^k + \theta^k d^k.$$

Here the search direction  $d^k$  is defined as

$$d^k = P_X (x^k - \alpha^k \nabla f(x^k)) - x^k,$$

where  $P_X$  denotes the orthogonal projection on  $X$ ,  $\alpha^k$  is obtained through the BB formula

$$\alpha_{BB}^k = \frac{\langle s^{k-1}, s^{k-1} \rangle}{\langle s^{k-1}, y^{k-1} \rangle}, \quad (11)$$

with  $s^{k-1} = x^k - x^{k-1}$  and  $y^{k-1} = \nabla f(x^k) - \nabla f(x^{k-1})$ , and the steplength  $\theta^k$  is such that the Grippo-Lampariello-Lucidi (GLL) condition [25] holds, i.e.,

$$\begin{aligned} & f(x^k + \theta^k d^k) \\ & \leq \max_{0 \leq j \leq \min\{k, \nu-1\}} f(x^{k-j}) + \gamma \theta^k \langle \nabla f(x^k), d^k \rangle \end{aligned} \quad (12)$$

with  $\nu \in \mathbb{N}$  and  $\gamma \in (0, 1)$ . More precisely, given a “small” parameter  $\alpha_{\min} > 0$  and a “large” parameter  $\alpha_{\max} > 0$ , the value of  $\alpha^k$  is set as

$$\alpha^k = \begin{cases} \min \{ \alpha_{\max}, \max \{ \alpha_{\min}, \alpha_{BB}^k \} \}, & \text{if } \alpha_{BB}^k > 0, \\ \alpha_{\max}, & \text{otherwise.} \end{cases} \quad (13)$$

A steplength  $\theta^k$  satisfying (12) is computed by a line search procedure, starting from the trial value  $\theta_0^k = 1$ . That is, if  $\theta_{j-1}^k$  is such that (12) does not hold, then a new candidate steplength  $\theta_j^k$  is computed by using a classical one-dimensional quadratic interpolation technique; furthermore, given the safeguard parameters  $\sigma_1$  and  $\sigma_2$ , with  $0 < \sigma_1 < \sigma_2 < 1$ , if  $\theta_j^k$  does not belong to  $[\sigma_1, \sigma_2 \theta_{j-1}^k]$ , then  $\theta_j^k = \theta_{j-1}^k / 2$ .

It can be proved that the SPG2 algorithm is convergent in the sense that any limit point  $\hat{x}$  of the sequence  $\{x^k\}$  generated by SPG2 is a stationary point of  $f$  in  $X$ , or equivalently

$$\|P_X(\hat{x} - \nabla f(\hat{x})) - \hat{x}\| = 0.$$

Our alternating minimization method based on SPG2 has the following structure: given  $(u^k, c_1^k, c_2^k)$  such that (9) holds, we first compute  $u^{k+1}$  by applying an SPG step to  $E(u, c_1^k, c_2^k)$  with  $(c_1^k, c_2^k)$  fixed, and then compute  $c_1^{k+1}$  and  $c_2^{k+1}$  by (9), using  $u^{k+1}$ . However, in the computation of  $u^{k+1} = u^k + \theta^k d_u^k$ , where  $d_u^k$  is the SPG search direction, we require that

$$\begin{aligned} & E(c_1^k, c_2^k, u^k + \theta^k d_u^k) \\ & \leq \max_{0 \leq j \leq \min\{k, \nu-1\}} E(c_1^{k-j}, c_2^{k-j}, u^{k-j}) \\ & \quad + \gamma \theta^k \langle G_u(c_1^k, c_2^k, u^k), d_u^k \rangle, \end{aligned} \quad (14)$$

i.e., we use a GLL condition that involves values of  $c_1$  and  $c_2$  different from the fixed ones  $c_1^k$  and  $c_2^k$  (unless  $\nu = 1$ ). On the other hand, since  $G_c(c_1^k, c_2^k, u^k) = 0$ , each iteration of the alternating minimization procedure can be regarded as the application of a projected gradient step to the function  $E$  with respect to all variables, followed by an “improvement” of the approximate solution resulting from that step. Furthermore,

**Algorithm 3.1** (SPGASeg)

---

given  $tol > 0$ ,  $\alpha_{max} > \alpha_{min} > 0$ ,  $\alpha^0 \in [\alpha_{min}, \alpha_{max}]$ ,  $0 < \sigma_1 < \sigma_2 < 1$ ,  $\nu \in \mathbb{N}$ ,  $\gamma \in (0, 1)$   
 choose  $u^0$  and compute  $c_1^0$  and  $c_2^0$  as in (9), using  $u^0$   
 set  $k = 0$   
**while**  $\|P_W(u^k - G_u(c_1^k, c_2^k, u^k)) - u^k\| > tol$  **do**  
   compute  $d_u^k = P_W(u^k - \alpha^k G_u(c_1^k, c_2^k, u^k)) - u^k$   
   compute  $\theta^k$  that satisfies (14) by a line search along  $u^k + \theta d_u^k$  and set  $u^{k+1} = u^k + \theta^k d_u^k$   
   compute  $c_1^{k+1}$  and  $c_2^{k+1}$  as in (9), using  $u^{k+1}$   
   compute  $\alpha^{k+1}$  according to (13) and (11), where  $s^k = u^{k+1} - u^k$  and  $y^k = G_u(c_1^{k+1}, c_2^{k+1}, u^{k+1}) - G_u(c_1^k, c_2^k, u^k)$   
   set  $k = k + 1$   
**end while**

---

letting  $d^k = (d_u^k, c_1^{k+1} - c_1^k, c_2^{k+1} - c_2^k)$ , the GLL condition holds with respect to all variables, i.e.,

$$\begin{aligned} E(c_1^{k+1}, c_2^{k+1}, u^{k+1}) \\ \leq \max_{0 \leq j \leq \min\{k, \nu-1\}} E(c_1^{k-j}, c_2^{k-j}, u^{k-j}) \\ + \gamma \theta^k \langle G(c_1^k, c_2^k, u^k), d^k \rangle, \end{aligned} \quad (15)$$

although  $(c_1^{k+1}, c_2^{k+1}, u^{k+1})$  is not obtained through a line search along  $d^k$ .

The SPG-based Alternating procedure described so far, henceforth referred to as SPGASeg (SPG-based Alternating procedure for Segmentation), is summarized in Algorithm 3.1, where  $W = [0, 1]^{mn}$ . Note that, since  $G_c(c_1^k, c_2^k, u^k) = 0$  for all  $k$ , the stopping condition reported in the algorithm is equivalent to

$$\|P_V((c_1^k, c_2^k, u^k) - G(c_1^k, c_2^k, u^k)) - (c_1^k, c_2^k, u^k)\| > tol,$$

where  $V = [u_{min}, u_{max}]^2 \times [0, 1]^{mn}$ . Furthermore, Algorithm SPGASeg differs from the inexact block coordinate descent methods presented in [7], because it does not satisfy conditions (3.5) in [7] and uses a nonmonotone line-search technique.

Now we prove that Algorithm SPGASeg preserves the convergence properties of SPG2. To this end, we first observe that for all  $(c_1, c_2, u) \in V$  and  $t \in (0, \alpha_{max}]$ ,

$$\begin{aligned} \langle G(c_1, c_2, u), G^t(c_1, c_2, u) \rangle \\ \leq -\frac{1}{t} \|G^t(c_1, c_2, u)\|^2 \\ \leq -\frac{1}{\alpha_{max}} \|G^t(c_1, c_2, u)\|^2, \end{aligned} \quad (16)$$

where the notation

$$\begin{aligned} G^t(c_1, c_2, u) &= P_V((c_1, c_2, u) - t G(c_1, c_2, u)) \\ &\quad - (c_1, c_2, u) \end{aligned}$$

has been used for simplicity. This is a known result (see [4, Lemma 2.1]), which follows straightforwardly

from the properties of the projection on a convex set (see, e.g., [3, Proposition 2.1.3, (b)]). In order to shorten the notation, we also define

$$G_u^t(c_1, c_2, u) = P_W(u - t G_u(c_1, c_2, u)) - u.$$

The convergence of Algorithm SPGASeg is stated in the following theorem.

**Theorem 1** *Algorithm SPGASeg is well defined and any limit point of the sequence  $\{(c_1^k, c_2^k, u^k)\}$  that it generates is a stationary point of  $E$  in  $V$ .*

*Proof* This proof closely follows the proof of Theorem 2.4 in [4], however we outline it for the sake of completeness.

If  $(c_1^k, c_2^k, u^k)$  is not a stationary point for  $E$  in  $V$ , then, by (16), for all  $t \in (0, \alpha_{max}]$  we have

$$\begin{aligned} \langle G(c_1^k, c_2^k, u^k), G^t(c_1^k, c_2^k, u^k) \rangle \\ \leq -\frac{1}{t} \|G^t(c_1^k, c_2^k, u^k)\|^2 \\ \leq -\frac{1}{\alpha_{max}} \|G^t(c_1^k, c_2^k, u^k)\|^2 < 0. \end{aligned}$$

It follows that

$$\begin{aligned} \langle G_u(c_1^k, c_2^k, u^k), d_u^k \rangle \\ = \langle G_u(c_1^k, c_2^k, u^k), G_u^t(c_1^k, c_2^k, u^k) \rangle < 0, \end{aligned}$$

because  $G_c(c_1^k, c_2^k, u^k) = 0$  for all  $k$ . Therefore,  $d_u^k$  is a descent direction for  $E(c_1^k, c_2^k, u)$  in  $u^k$ , and a step-size  $\theta^k$  such that (14) holds can be computed with a finite number of trials. Thus, Algorithm SPGASeg is well defined.

Now we suppose that  $(\hat{c}_1, \hat{c}_2, \hat{u}) \in V$  is a limit point of the sequence generated by Algorithm SPGASeg. Without loss of generality, we can assume that the sequence

$\{(c_1^k, c_2^k, u^k)\}$  converges to  $(\hat{c}_1, \hat{c}_2, \hat{u})$ . We distinguish two cases.

*Case 1:*  $\inf \theta^k = 0$ .

By contradiction we suppose that  $(\hat{c}_1, \hat{c}_2, \hat{u})$  is not a stationary point, i.e.,  $G^\alpha(\hat{c}_1, \hat{c}_2, \hat{u}) \neq 0$  for all  $\alpha > 0$ . From  $G_c(c_1^k, c_2^k, u^k) = 0$  it follows that  $G_c(\hat{c}_1, \hat{c}_2, \hat{u}) = 0$  and hence  $G_u^\alpha(\hat{c}_1, \hat{c}_2, \hat{u}) \neq 0$ . Then, by reasoning as in the proof of Theorem 2.4 in [4], we find that there exists  $\delta > 0$  such that for all sufficiently large  $k$ ,

$$\left\langle G_u(c_1^k, c_2^k, u^k), \frac{G_u^\alpha(c_1^k, c_2^k, u^k)}{\|G_u^\alpha(c_1^k, c_2^k, u^k)\|} \right\rangle < -\frac{\delta}{2}, \quad (17)$$

for all  $\alpha \in [\alpha_{\min}, \alpha_{\max}]$ .

Since  $\inf \theta^k = 0$ , there exists  $K \subseteq \mathbb{N}$  such that

$$\lim_{k \in K} \theta^k = 0.$$

Then, moving from the way  $\theta^k$  is chosen to satisfy the GLL condition (14) and proceeding again as in [4], we find that for all sufficiently large  $k \in K$ , there exists  $\rho^k$ , with  $0 < \sigma_1 \leq \rho^k \leq \sigma_2$ , and  $t^k \in [0, \theta^k / \rho^k]$  such that

$$\langle G_u(c_1^k, c_2^k, u^k + t^k d_u^k), d_u^k \rangle > \gamma \langle G_u(c_1^k, c_2^k, u^k), d_u^k \rangle.$$

Hence, by taking a subsequence  $\{d_u^k\}_{k \in K_1 \subseteq K}$  such that  $d_u^k / \|d_u^k\|$  is convergent with limit  $\hat{d}_u$ , we get

$$\langle G_u(\hat{c}_1, \hat{c}_2, \hat{u}), \hat{d}_u \rangle = 0.$$

From  $d_u^k = G_u^{\alpha^k}(c_1^k, c_2^k, u^k)$  it follows, by continuity, that for all sufficiently large  $k \in K_1$ ,

$$\left\langle G_u(c_1^k, c_2^k, u^k), \frac{G_u^{\alpha^k}(c_1^k, c_2^k, u^k)}{\|G_u^{\alpha^k}(c_1^k, c_2^k, u^k)\|} \right\rangle > -\frac{\delta}{2},$$

which contradicts (17).

*Case 2:*  $\inf \theta^k \geq \rho > 0$ .

By contradiction, we suppose that  $(\hat{c}_1, \hat{c}_2, \hat{u})$  is not a constrained stationary point. Then  $\|G^\alpha(\hat{c}_1, \hat{c}_2, \hat{u})\| > 0$  for all  $\alpha \in (0, \alpha_{\max}]$  and hence there exists  $\delta > 0$  such that  $\|G^\alpha(\hat{c}_1, \hat{c}_2, \hat{u})\| \geq \delta$  for all  $\alpha \in [\rho, \alpha_{\max}]$ .

Let  $l(k)$  be an integer such that  $k - \min\{k, \nu - 1\} \leq l(k) \leq k$  and

$$\begin{aligned} E(c_1^{l(k)}, c_2^{l(k)}, u^{l(k)}) \\ = \max_{0 \leq j \leq \min\{k, \nu-1\}} E(c_1^{k-j}, c_2^{k-j}, u^{k-j}). \end{aligned}$$

By reasoning as in the proof of Theorem 2.4 in [4], we find that  $\{E(c_1^{l(k)}, c_2^{l(k)}, u^{l(k)})\}$  is a nonincreasing sequence; furthermore, for  $k$  sufficiently large, we have

$$\|G^\alpha(c_1^{l(k)}, c_2^{l(k)}, u^{l(k)})\| \geq \delta/2.$$

Then, by (15) and (16), we get

$$\begin{aligned} E(c_1^{l(k)}, c_2^{l(k)}, u^{l(k)}) \\ \leq E(c_1^{l(k)-1}, c_2^{l(k)-1}, u^{l(k)-1}) \\ - \frac{\gamma \rho}{\alpha_{\max}} \left\| G^{\alpha^{l(k)-1}}(c_1^{l(k)-1}, c_2^{l(k)-1}, u^{l(k)-1}) \right\|^2 \\ \leq E(c_1^{l(k)-1}, c_2^{l(k)-1}, u^{l(k)-1}) - \frac{\gamma \delta^2 \rho}{4 \alpha_{\max}}. \end{aligned}$$

It follows that

$$\lim_{k \rightarrow \infty} E(c_1^{l(k)}, c_2^{l(k)}, u^{l(k)}) = -\infty,$$

which is a contradiction because, by continuity,

$$\lim_{k \rightarrow \infty} E(c_1^{l(k)}, c_2^{l(k)}, u^{l(k)}) = E(\hat{c}_1, \hat{c}_2, \hat{u}).$$

This completes the proof.  $\square$

It is worth noting that Algorithm SPGASeg can be applied in a more general context than the one considered in this work. More precisely, let  $X \times Y \subset \mathbb{R}^p \times \mathbb{R}^q$  be a closed convex set and  $F(x, y)$  a real-valued function that is continuously differentiable in an open set containing  $X \times Y$ . If we assume that for all  $y \in Y$   $\arg\min_{x \in X} F(x, y)$  exists and can be exactly computed, then we can apply Algorithm SPGASeg to  $F(x, y)$ , with  $x$  playing the role of  $(c_1, c_2)$  and  $y$  the role of  $u$ . Of course, the convergence of the algorithm still holds.

## 4 Computational experiments

We performed numerical experiments to evaluate the effectiveness of our approach. To this aim, we applied the Algorithm SPGASeg to several gray-scale images with different sizes and features, which are widely used in the literature of image segmentation. For the sake of space, we report only the results concerning six images, showing either real scenes or synthetic pictures, which are representative of the general behaviour of the proposed method (see the first column in Figures 1-2).

Algorithm SPGASeg was implemented in C, in single precision, exploiting the implementation of Algorithm SPG2 [5] available as a part of the TANGO project (<http://www.ime.usp.br/~egbirgin/tango/>). It was run under Matlab (R2011b, v. 7.13), through a MEX-interface, using the Image Processing Toolbox to read and display images. The C code was compiled by using gcc (v. 4.7.2) and the experiments were performed on an Intel Core i5 processor with clock frequency of 2.7 GHz and 8 GB of RAM.

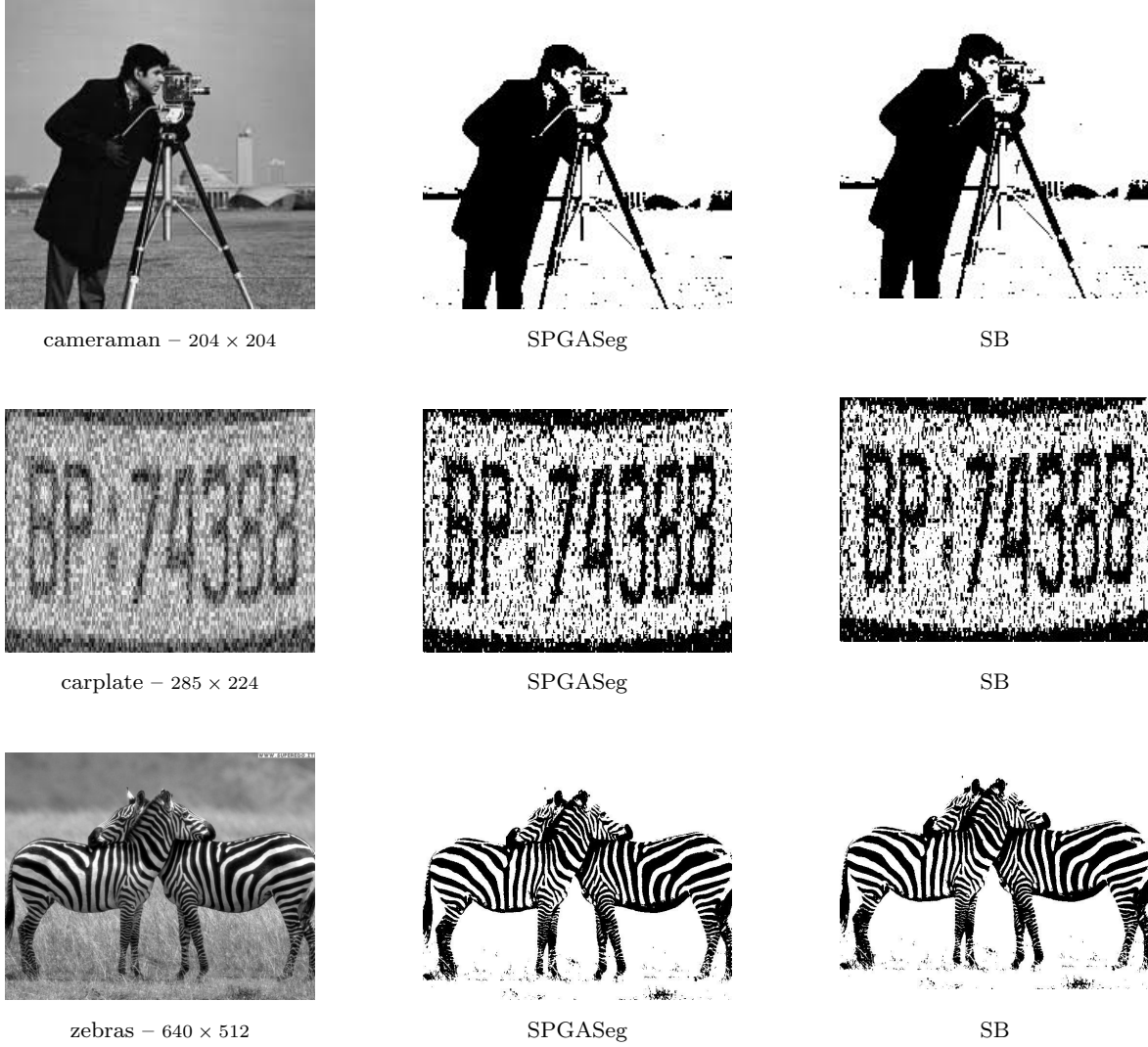


**Fig. 1** Real scenes and corresponding segmentations by SPGASeg and SB. The number of pixels of each image is specified after the name. The images have been resized using different scalings to fit the figure layout.

The parameters in the objective function  $E(c_1, c_2, u)$  were set as  $\lambda = 0.5$  and  $\varepsilon = 10^{-6}$ , and the threshold parameter in (6) as  $\mu = 0.5$ . Following the implementation of SPG2, the  $\ell_\infty$  norm was used instead of the  $\ell_2$  norm in the SPGASeg stopping criterion, with  $tol = 10^{-6}$ . A maximum number of iterations equal to 1000 and a maximum number of function evaluations equal to 10000 were also considered. The values  $\nu = 10$  and  $\gamma = 10^{-4}$  were used in the GLL condition (14). The parameters  $\alpha_{min}$ ,  $\alpha_{max}$ ,  $\sigma_1$  and  $\sigma_2$  were left equal to their default values in SPG2. The initial value of  $\alpha$  was also chosen as in SPG2, i.e.,  $\alpha^0 = \min\{\alpha_{max}, \max\{\alpha_{min}, 1/\|G_u^1(c_1^0, c_2^0, u^0)\|_\infty\}\}$ .

For each test problem we used three choices of the initial function  $u^0$ :

- $\bar{u}_{[0,1]}$ , the image to be segmented, with intensity values scaled between 0 and 1;
- $u_{ws}$ , a small white square ( $p \times q$  pixels, with  $p \ll m$  and  $q \ll n$ ) on black background;
- $u_{bs}$ , a small black square ( $p \times q$  pixels, with  $p \ll m$  and  $q \ll n$ ) on white background.

Since the three functions led to the same segmentations, we report here the results obtained by choosing  $u^0 = \bar{u}_{[0,1]}$ .

For comparison purpose, we also applied to the CEN model the SPG2 algorithm and the SB-based algorithm described in [23], for all the test problems. The former was chosen to evaluate the behaviour of our approach with respect to a straightforward application of the spectral projected gradient algorithm; the latter is

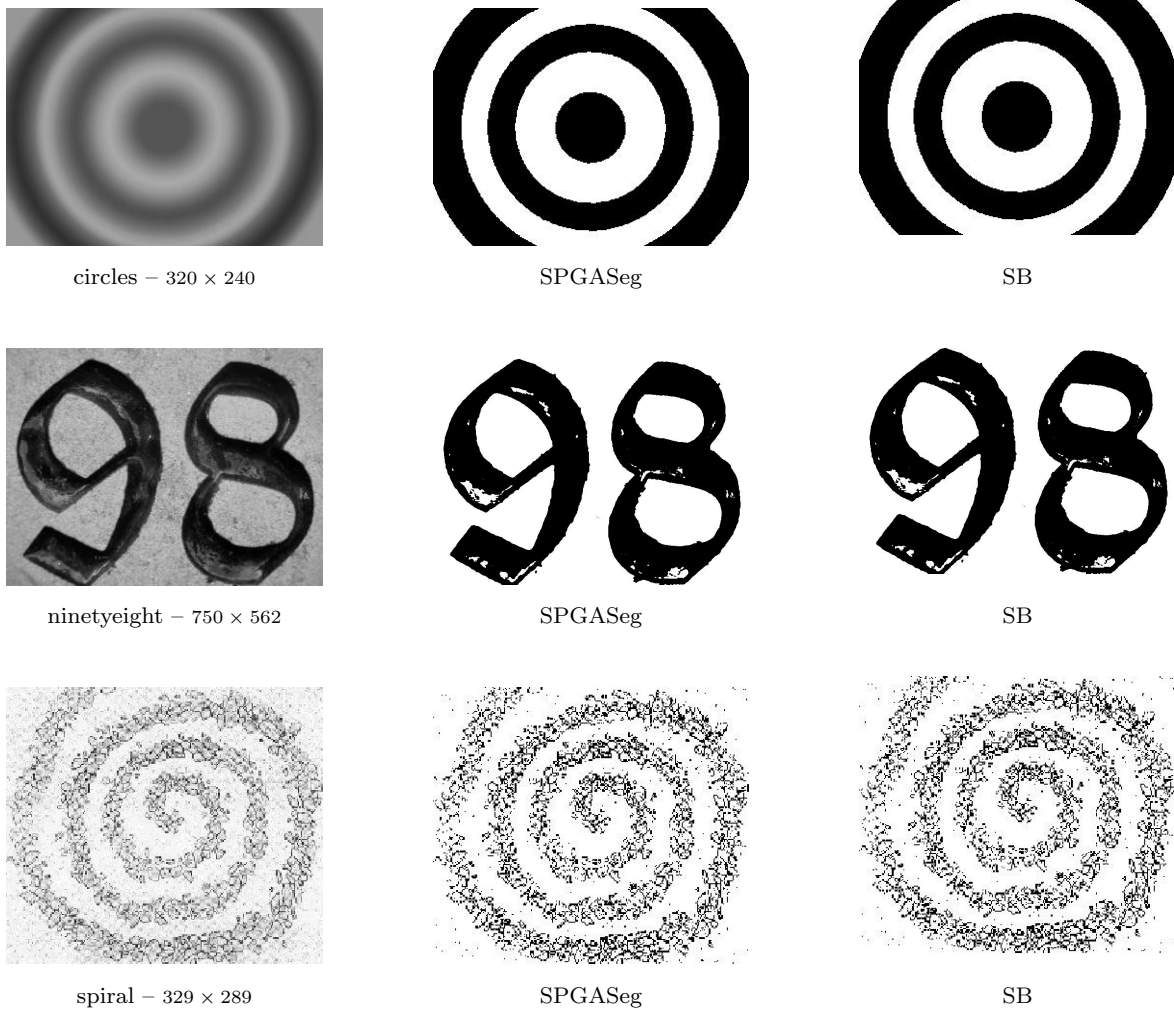


**Fig. 2** Synthetic pictures and corresponding segmentations by SPGASeg and SB. The number of pixels of each image is specified after the name. The images have been resized using different scalings to fit the figure layout.

known to be very efficient and therefore it was taken as a reference algorithm for our analysis. The SB approach computes an approximation  $u^{k+1}$  to  $u$  by performing the following steps:

$$(u^{k+1}, d^{k+1}) = \underset{0 \leq u \leq 1; d}{\operatorname{argmin}} \int_{\Omega} \left( |d| + \lambda u r + \frac{\eta}{2} |d - \nabla u - b^k|^2 \right) dx, \quad (18)$$

$$b^{k+1} = b^k + \nabla u^k - d^k, \quad (19)$$

where  $r = (c_1 - \bar{u})^2 - (c_2 - \bar{u})^2$ . Problem (18) is approximately solved by an alternating minimization procedure, where  $u^{k+1}$  is obtained by applying the Gauss-Seidel method to the Euler-Lagrange equations (with  $d = d^k$ ) and projecting the computed solution in  $[0, 1]$ , while  $d^{k+1}$  is obtained by applying the so-called shrink operator (see [23] for more details).

A single precision version of the aforementioned implementation of SPG2 was used in the experiments,

with the same values of the parameters as in the SPGASeg code. Concerning the SB approach, the implementation available from <http://www.xavier-bresson.tk> was applied. This is a single-precision C code with a MEX interface, allowing to run it under Matlab. Its native stopping criterion for the outer iterations was substituted by the stopping criterion used in SPGASeg and SPG2, in order to make a fair comparison. The parameter  $\eta$  in (18) was set equal to 1; the stopping criterion for the Gauss-Seidel iterations remained unchanged.

Details about the behaviour of SPGASeg, SPG2 and SB are given in Table 1. For all the algorithms we show the number of iterations,  $nit$ , performed to satisfy the stopping criterion. For SPGASeg and SPG2 we also show the number,  $nf$ , of objective function evaluations, each requiring  $O(mn)$  floating-point operations.



IMAGE	SPGASeg		SPG2		SB	
	$nit$	$nf$	$nit$	$nf$	$nit$	$n_{GS}$
cameraman	5	11	72	104	5	10
carplate	3	7	118	209	4	8
zebras	5	11	336	571	5	10
circles	3	7	44	53	3	6
ninetyeight	3	7	168	309	4	8
spiral	6	13	454	788	7	14
noisy cameraman	7	15	283	527	8	16
noisy ninetyeight	5	11	—	—	5	10

**Table 1** Details about the execution of SPGASeg, SPG2 and SB on the selected test problems (“—” indicates that the required accuracy has not been achieved within the maximum number of iterations).

The number of gradient evaluations, which costs  $O(mn)$  floating-point operations plus the computation of the square roots in (8), is not reported since it is equal to the number of iterations plus 1. For the SB algorithm we also show the number,  $n_{GS}$ , of Gauss-Seidel iterations, each performing  $O(mn)$  floating-point operations. The number of updates of  $d^{k+1}$  and  $b^{k+1}$  is equal to  $n_{GS}$  (each update is again  $O(mn)$ ).

We see that SPGASeg is much more efficient than SPG2. SPGASeg generally achieves the required accuracy in at most 7 iterations, with at most 15 objective function evaluations, while SPG2 requires a much larger number of iterations and objective function evaluations. This behaviour is more evident for images with a particular texture, such as “zebras” or “ninetyeight”, or corrupted by a large amount of noise, such as “carplate” and “spiral”. The large increase in the number of SPG2 iterations because of noise is confirmed by further numerical experiments, performed adding noise to some images. For example, in the last two rows of Table 1 we report the results obtained after corrupting the real image “cameraman” and the synthetic one “ninetyeight” with Gaussian noise having zero mean and standard deviation values of 15 and 25, respectively (the corrupted images are shown in the left column of Figure 3). We see that the noise strongly deteriorates the performance of SPG2, while it slightly affects the behaviour of SPGASeg (note that SPG2 does not achieve the required accuracy within the maximum number of iterations on the “noisy ninetyeight” image).

Conversely, the SPGASeg and SB algorithms perform about the same number of iterations and show similar time complexity for all the test images. In order to evaluate more completely the efficiency of our approach, we also compare the execution time of the SPGASeg code with that of the SB one. These times, obtained as average values over 20 runs, are reported in Table 2. Note that the time measurement of SB does not

IMAGE	SPGASeg	SB
cameraman	0.013	0.009
carplate	0.014	0.015
zebras	0.112	0.078
circles	0.016	0.010
ninetyeight	0.092	0.074
spiral	0.037	0.036
noisy cameraman	0.018	0.016
noisy ninetyeight	0.144	0.098

**Table 2** Execution times (seconds) of SPGASeg and SB on the selected test problems.

include the gradient evaluations needed by the modified stopping criterion introduced in that code for comparison purpose. We see that for “carplate”, “spiral” and “noisy cameraman” the times of SPGASeg and SB are comparable, while for the other images SB is slightly faster. This is a satisfactory result, since the SB method is known to be very efficient on the segmentation model considered in this paper. Furthermore, we think that our implementation of SPGASeg can be improved to enhance its performance; however, this issue is beyond the scope of this article.

Finally, we highlight that the segmentations obtained using SPGASeg and SB are the same, for both the images of the original test set and those obtained by adding Gaussian noise (see the second and third column of Figures 1-3). In particular, the small amount of regularization introduced in the TV term does not affect the results. The quality of the segmentations is generally good, since the “meaningful” regions of each image are identified.

## 5 Conclusions

We presented an alternating minimization procedure called SPGASeg, which exploits the nonmonotone SPG method for solving the formulation of segmentation problems provided by the CEN model. The choice of the SPG method was motivated by its steplength selection strategy, allowing faster convergence than classical gradient methods.

We proved that Algorithm SPGASeg is globally convergent to a constrained stationary point of the discretized CEN model. Numerical experiments on images widely used in the image segmentation literature showed that SPGASeg is able to solve problem (10) with a small number of iterations, producing segmentations equal to those obtained with the SB algorithm presented in [23], which is very effective on the model considered in this work. Furthermore, the efficiency of

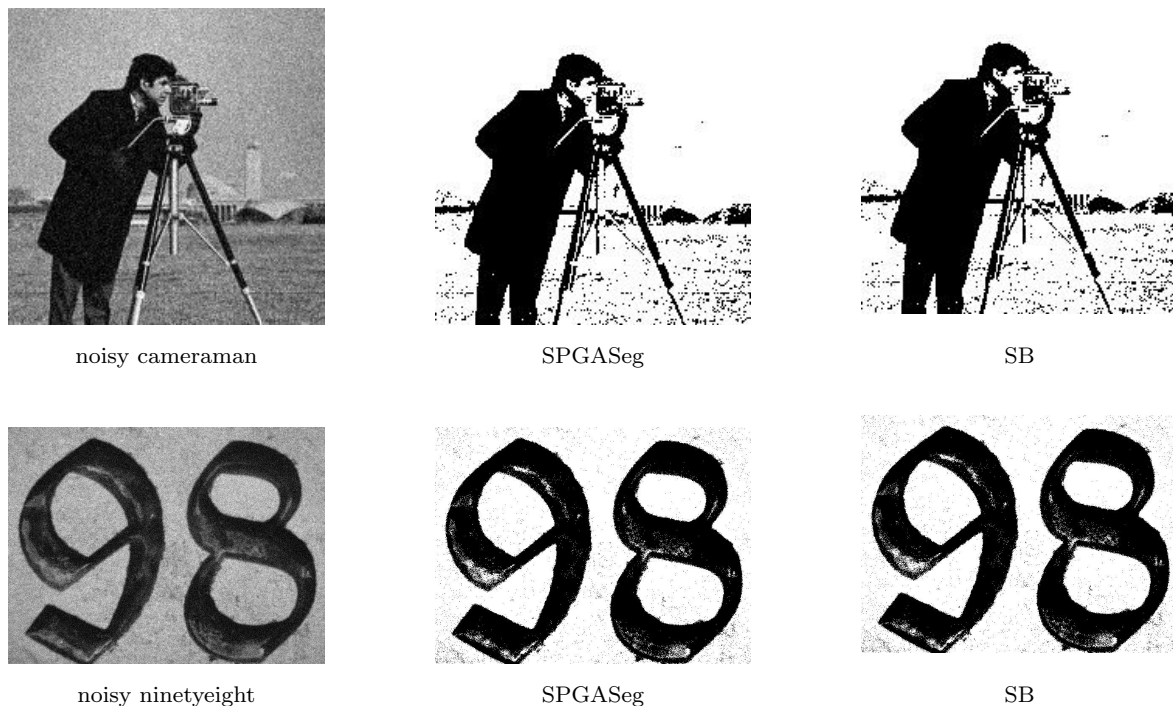


**Fig. 3** Images corrupted by Gaussian noise and corresponding segmentations by SPGASeg and SB.

SPGASeg in terms of execution time appeared to be satisfactory.

Finally, our work shows that projected gradient methods with suitable line search techniques can be effectively exploited in the context of variational image segmentation.

**Acknowledgements** We wish to thank Giovanni Pisante for useful discussions concerning variational models for image segmentation. We are also grateful to the anonymous referees for their useful comments, which helped us to improve the quality of this work.

## References

1. Aujol, J.F., Chambolle, A.: Dual norms and image decomposition models. *International Journal of Computer Vision* **63**(1), 85–104 (2005)
2. Barzilai, J., Borwein, J.: Two-point step size gradient methods. *IMA Journal of Numerical Analysis* **8**, 141–148 (1988)
3. Bertsekas, D.: *Nonlinear Programming*, 2nd edn. Athena Scientific, Belmont, MA, USA (1999)
4. Birgin, E., Martínez, J., Raydan, M.: Nonmonotone spectral projected gradient methods on convex sets. *SIAM Journal on Optimization* **10**(4), 1196–1211 (2000)
5. Birgin, E., Martínez, J., Raydan, M.: Algorithm 813: SPG – software for convex-constrained optimization. *ACM Transactions on Mathematical Software* **27**(3), 340–349 (2001)
6. Birgin, E., Martínez, J., Raydan, M.: Spectral projected gradient methods: review and perspectives. *Journal of Statistical Software* **60**(3) (2014)
7. Bonettini, S.: Inexact block coordinate descent methods with application to non-negative matrix factorization. *IMA Journal of Numerical Analysis* **31**(4), 1431–1452 (2011)
8. Bonettini, S., Zanella, R., Zanni, L.: A scaled gradient projection method for constrained image deblurring. *Inverse Problems* **25**(1), 015,002 (25 pp.) (2009)
9. Bresson, X., Esedoglu, S., Vandergheynst, P., Thiran, J.P., Osher, S.: Fast global minimization of the active contour/snake model. *Journal of Mathematical Imaging and Vision* **28**(2), 151–167 (2007)
10. Brown, E., Chan, T., Bresson, X.: Completely convex formulation of the Chan–Vese image segmentation model. *International Journal of Computer Vision* **98**(1), 103–121 (2012)
11. Chambolle, A.: An algorithm for total variation minimization and applications. *Journal of Mathematical Imaging and Vision* **20**(1–2), 89–97 (2004)
12. Chambolle, A., Pock, T.: A first-order primal-dual algorithm for convex problems with applications to imaging. *Journal of Mathematical Imaging and Vision* **40**(1), 120–145 (2011)
13. Chan, T., Esedoglu, S., Nikolova, M.: Algorithms for finding global minimizers of image segmentation and denoising models. *SIAM Journal on Applied Mathematics* **66**(5), 1632–1648 (2006)
14. Chan, T., Sandberg, B., Moelich, M.: Some recent developments in variational image segmentation. In: X.C. Tai, K.A. Lie, T. Chan, F. Osher (eds.) *Image Processing based on Partial Differential Equations*, Mathematics

- and Visualization Series, pp. 175–201. Springer, Heidelberg (2005)
15. Chan, T., Vese, L.: Active contours without edges. *IEEE Transactions on Image Processing* **10**(2), 266–277 (2001)
16. Dai, Y.H., Fletcher, R.: Projected Barzilai–Borwein methods for large-scale box-constrained quadratic programming. *Numerische Mathematik* **100**(1), 21–47 (2005)
17. Dai, Y.H., Yuan, Y.: Analysis of monotone gradient methods. *Journal of Industrial and Management Optimization* **1**(2), 181–192 (2005)
18. De Asmundis, R., di Serafino, D., Hager, W., Toraldo, G., Zhang, H.: An efficient gradient method using the Yuan steplength. *Computational Optimization and Applications* **59**(3), 541–563 (2014)
19. De Asmundis, R., di Serafino, D., Riccio, F., Toraldo, G.: On spectral properties of steepest descent methods. *IMA Journal of Numerical Analysis* **33**(4), 1416–1435 (2013)
20. Esser, E.: Applications of Lagrangian-based alternating direction methods and connections to split Bregman. CAM Technical Report 09-31, UCLA, Los Angeles, CA, USA, available from <ftp://ftp.math.ucla.edu/pub/camreport/cam09-31.pdf> (2009)
21. Figueiredo, M., Nowak, R., Wright, S.: Gradient projection for sparse reconstruction: application to compressed sensing and other inverse problems. *IEEE Journal of Selected Topics in Signal Processing* **1**(4), 586–598 (2007)
22. Fletcher, R.: A limited memory steepest descent method. *Mathematical Programming, Series A* **135**(1–2), 413–436 (2012)
23. Goldstein, T., Bresson, X., Osher, S.: Geometric applications of the split Bregman method: segmentation and surface reconstruction. *Journal of Scientific Computing* **45**(1–3), 272–293 (2010)
24. Goldstein, T., Osher, S.: The split Bregman method for  $l_1$ -regularized problems. *SIAM Journal on Imaging Sciences* **2**(2), 323–343 (2009)
25. Grippo, L., Lampariello, F., Lucidi, S.: A nonmonotone line search technique for Newton’s method. *SIAM Journal on Numerical Analysis* **23**(4), 707–716 (1986)
26. Jung, M., Kang, M., Kang, M.: Variational image segmentation models involving non-smooth data-fidelity terms. *Journal of Scientific Computing* **59**(2), 277–308 (2014)
27. Mumford, D., Shah, J.: Optimal approximations by piecewise smooth functions and associated variational problems. *Communications on Pure and Applied Mathematics* **45**(2), 577–685 (1989)
28. Papadakis, N., Yildizoglu, R., Aujol, J.F., Caselles, V.: High-dimension multilabel problems: Convex or nonconvex relaxation? *SIAM Journal on Imaging Sciences* **6**(4), 2603–2639 (2013)
29. Setzer, S.: Operator splittings, Bregman methods and frame shrinkage in image processing. *International Journal of Computer Vision* **92**(3), 265–280 (2011)
30. Wang, Y., Yang, J., Yin, W., Zhang, Y.: A new alternating minimization algorithm for total variation image reconstruction. *SIAM Journal on Imaging Sciences* **1**(3), 248–272 (2008)
31. Yildizoglu, R., Aujol, J.F., Papadakis, N.: Active contours without level sets. In: *ICIP 2012 – IEEE International Conference on Image Processing* (Orlando, FL, Sept. 30 – Oct. 3, 2012), pp. 2549–2552. IEEE (2012)
32. Yu, G., Qi, L., Dai, Y.H.: On nonmonotone Chambolle gradient projection algorithms for total variation image restoration. *Journal of Mathematical Imaging and Vision* **35**(2), 143–154 (2005)
33. Zhu, M., Wright, S., Chan, T.: Duality-based algorithms for total-variation-regularized image restoration. *Computational Optimization and Applications* **47**(3), 377–400 (2010)